Available online at www.sciencedirect.com
SCIENCE DIRECT
International Journal of Heat and Mass Transfer 49 (2006) 89–96
International Journal of HEAT and MASS TRANSFER
www.elsevier.com/locate/ijhmt

# The effect of stable thermal stratification on the onset of double-diffusive convection in electrochemical systems

Min Chan Kim [a,*], Sang Baek Lee [a], Sin Kim [b], Bum-Jin Chung [b]

[a] Department of Chemical Engineering, Cheju National University, Cheju 690-756, Republic of Korea
[b] Department of Nuclear and Energy Engineering, Cheju National University, Cheju 690-756, Republic of Korea

Received 2 December 2004; received in revised form 4 August 2005
Available online 3 October 2005

**Abstract**

The onset time of double-diffusive convection in time-dependent, nonlinear concentration fields was investigated theoretically and experimentally. The stability analysis was conducted on the basis of the propagation theory. Under the linear stability theory, the linearized perturbation equations were transformed similarly by using the concentration penetration depth as a length-scaling factor. The newly derived stability equations were solved numerically. Also the onset time was determined experimentally by employing an electrochemical technique where 0.03–0.3 M $CuSO_4$ + 1.5 M $H_2SO_4$ aqueous solutions were adopted as electrolyte. The onset time of double-diffusive convection was delayed or shortened depending on the degree of stable stratification.


*Keywords:* Buoyancy-driven instability; Onset time; Double diffusion; Stable thermal stratification; Propagation theory; Electrochemical experiment

## 1. Introduction

Buoyancy-driven convection in double-diffusive systems has been studied extensively in connection with wide engineering applications such as crystal growth processing, solar ponds and natural gas storage tanks [1–3]. It will enhance or reduce heat and/or mass transfer rates, of which magnitude depends on the direction of the temperature and concentration gradients and the ratio of thermal to solutal diffusivity. But the inherent complexity in convective transport phenomena makes it very difficult to predict the critical condition, the onset of double-diffusive convection.

In an initially motionless, stably thermally stratified fluid layer placed between two horizontal plates where the concentration field changes suddenly, natural convection will set in at a certain time, depending on both the thermal Rayleigh number and the solute Rayleigh number. Nield [4] examined the linear stability theory to obtain the onset conditions of thermohaline convection in horizontal fluid layer. Turner [2] summarized stability conditions of double-diffusive systems. Kaviany and Vogel [5], and Yoon et al. [6] analyzed the stability conditions of double-diffusive system under the nonlinear, time-dependent temperature gradient by employing their amplification theory and propagation theory, respectively. The amplification theory is quite popular

* Corresponding author. Tel.: +82 64 754 3685; fax: +82 64 755 3670.
*E-mail address:* mckim@cheju.ac.kr (M.C. Kim).

0017-9310/$ - see front matter © 2005 Elsevier Ltd. All rights reserved.
doi:10.1016/j.ijheatmasstransfer.2005.08.004

**Nomenclature**

| | |
|---|---|
| $a$ | dimensionless wave number |
| $C$ | concentration [M] |
| $d$ | fluid layer thickness [m] |
| $g$ | gravitation acceleration [m/s$^2$] |
| $Le$ | Lewis number, $\alpha/\alpha_s$ |
| $Ra$ | Rayleigh number, $g\beta\Delta T d^3/(\alpha v)$ |
| $Rs$ | solutal Rayleigh number, $g\beta_s\Delta T d^3/(\alpha_s v)$ |
| $Sc$ | Schmidt number, $v/\alpha_s$ |
| $T$ | temperature [K] |
| $(u,v,w)$ | dimensionless velocity disturbances in Cartesian coordinates |
| $(x,y,z)$ | dimensionless Cartesian coordinates |

*Greek symbols*

| | |
|---|---|
| $\alpha$ | thermal diffusivity [m$^2$/s] |
| $\alpha_s$ | mass diffusivity [m$^2$/s] |
| $\beta$ | volumetric thermal expansion coefficient [K$^{-1}$] |
| $\beta_s$ | volumetric solutal expansion coefficient [M$^{-1}$] |
| $\Delta_c$ | concentration boundary layer thickness [m] |
| $\delta_c$ | dimensionless concentration boundary layer thickness, $\Delta_c/d$ |
| $\zeta$ | dimensionless similarity variable, $z/\tau^{1/2}$ |
| $\theta$ | dimensionless temperature disturbance, $g\beta d^3 T_1/(\alpha v)$ |
| $\theta_0$ | dimensionless basic temperature, $(T_0 - T_i)/\Delta T$ |
| $\phi$ | dimensionless concentration disturbance, $g\beta_s d^3 C_1/(\alpha_s v)$ |
| $\phi_0$ | dimensionless basic concentration, $C_0/\Delta C$ |
| $v$ | kinematic viscosity [m$^2$/s] |
| $\tau$ | dimensionless time |
| $\rho$ | density [kg/m$^3$] |

*Subscripts*

| | |
|---|---|
| 0 | basic quantities |
| 1 | perturbation quantities |
| c | critical conditions |

*Superscript*

| | |
|---|---|
| * | transformed quantities |

but it requires both the initial conditions and the amplification factor to mark manifest buoyancy-driven motion [5,7,8]. The propagation theory employs the thermal penetration depth as a length scaling factor and then the linearized equations are transformed into the similar forms [9–11]. This theory has produced the critical conditions comparable with experimental measurements. The propagation has been extended to the system of solidification [12] and surface-tension driven convection [13,14] and onset of Taylor-like vortices in the various systems [15–17].

In the present study, the onset of double-diffusive convection is analyzed theoretically and experimentally. The effect of stable thermal stratification on the onset of double-diffusive convection is analyzed by employing propagation theory. And the validity of theoretical results is discussed in comparison with experimental results in electrochemical ionic mass transfer system.

## 2. Theoretical analysis

### 2.1. Mathematical formulations

The problem considered here is a horizontal fluid layer confined between two rigid boundaries separated by a distance $d$, as shown in Fig. 1. The fluid layer is initially quiescent at a constant concentration $C_i$ and stably stratified by a uniform temperature gradient. At time

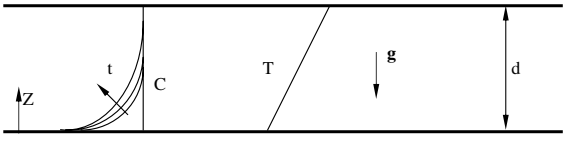


Fig. 1. Schematic diagram of system considered here.

$t = 0$ the concentration of the lower boundary is reduced and kept constant. For large concentration difference systems natural convection will set in at a certain time due to buoyancy force. Under this condition the density variation of fluid is assumed to follow the usual equation of state [2]:

$$\rho = \rho_r[1 - \beta(T - T_r) + \beta_s(C - C_r)], \tag{1}$$

where $\rho$, $T$, $C$, $\beta$ and $\beta_s$ represent fluid density, temperature, concentration, thermal expansion coefficient and solutal expansion coefficient, respectively. The subscript "0" denotes the reference state.

The important parameters to characterize the onset of motion in the present system are solutal Rayleigh number $Rs$, thermal Rayleigh number $Ra$, Schmidt number $Sc$ and Lewis number $Le$ defined by

$$Ra = \frac{g\beta\Delta T d^3}{\alpha v}, \quad Rs = \frac{g\beta_s\Delta C d^3}{\alpha_s v},$$

$$Sc = \frac{v}{\alpha_s} \quad \text{and} \quad Le = \frac{\alpha}{\alpha_s},$$

where $g$, $\alpha$, $\nu$, $\Delta T$, $\alpha_s$ and $\Delta C$ denote gravitational acceleration, thermal diffusivity, kinematic viscosity, temperature difference, mass diffusivity and concentration difference, respectively. Under the linear stability theory, the nondimensionalized conservation equations are given as:

$$\left(\frac{1}{Sc}\frac{\partial}{\partial\tau}-\nabla^2\right)\nabla^2 w=\nabla_1^2\phi_1-Le\nabla_1^2\theta_1, \tag{2}$$

$$\frac{\partial\phi_1}{\partial\tau}+Rs\frac{\partial\phi_0}{\partial z}w=\nabla_1^2\phi_1, \tag{3}$$

$$\frac{\partial\theta_1}{\partial\tau}+Ra\frac{\partial\theta_0}{\partial z}w=Le\nabla_1^2\theta_1, \tag{4}$$

under the following boundary conditions:

$$w_1=\frac{\partial w_1}{\partial z}=\phi_1=\theta_1=0 \quad \text{at } z=0 \text{ and } z=1. \tag{5}$$

Here, $\nabla^2$ is the three-dimensional Laplacian, and $\nabla_1^2$ is the horizontal one with respects to $x$ and $y$. Here $z$, $\tau$, $w_1$, $\theta_0$, $\theta_1$, $\phi_0$ and $\phi_1$ are the dimensionless vertical distance, time, basic temperature, perturbed temperature, basic concentration and perturbed concentration, respectively. Each variable has been nondimensionalized by using $d$, $d^2/\alpha_s$, $\alpha_s/d$, $\Delta T$, $\alpha\nu/g\beta d^3$, $\Delta C$ and $\alpha_s\nu/g\beta_s d^3$, respectively.

For the deep-pool system of small $\tau$, the basic concentration field is given as

$$\phi_0=\mathrm{erf}\left(\frac{z}{2\sqrt{\tau}}\right). \tag{6}$$

For the thermally stably stratified fluid layer, the dimensionless temperature field is linear as shown in Fig. 1. Therefore the basic density field satisfying the equation of state can be defined as

$$\bar{\rho}=\phi_0-\frac{RaLe}{Rs}\theta_0, \tag{7}$$

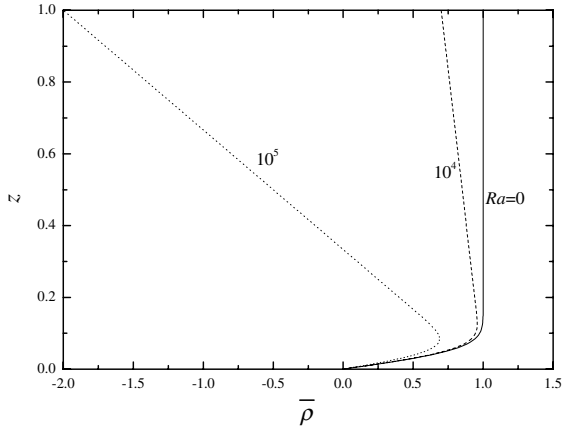


Fig. 2. Base density profiles with respect $Ra$ for $Rs=10^7$, $Le=300$ and $\tau=10^{-3}$.

where $\bar{\rho}$ denotes the nondimensionalized basic density defined as $(\rho-\rho_r)\Delta C\beta_s/\rho_r$. The resultant variation of the profile of the basic density is shown in Fig. 2 where maximum magnitude of density locates within the fluid layer.

### 2.2. Propagation theory

For the given $Rs$, $Sc$, $Ra$ and $Le$ the time to mark the onset of convective motion is to be found under the principle of exchange of stabilities from Eqs. (2)–(4), subjected to the boundary conditions of Eq. (5). Even though the initially stratified density field may reduce the magnitude of the generated disturbances, the disturbances are to be generated continuously. Hence, the density distribution for molecular diffusion of heat and mass in aqueous solution becomes time-dependent. It is a formidable task to obtain quantitative estimates of the onset time of the double-diffusive convection. In the frozen-time model the terms involving $\partial(\cdot)/\partial\tau$ are neglected and therefore the system becomes time-independent. The proper initial conditions at $\tau=0$ are required in the stochastic model and the amplification theory. Among the models the amplification theory is quite popular but its amplification factor to represent manifest convection should be decided experimentally. The propagation theory described below is a rather simple, deterministic approach and it will be employed here for the stability analysis.

The propagation theory employed for finding the critical time $t_c$ is based on the assumption that disturbances at the onset of convection are mainly confined within the solutal penetration depth $\Delta_c$. For small $t$ the following relation is obtained from the balance between the viscous and buoyant forces in the $z$-component of motion from Eq. (2)

$$\left|\frac{w_1}{\phi_1}\right|\sim\delta_c^2\sim\tau, \tag{8}$$

where $\delta_c(\propto\sqrt{\tau})$ is the dimensionless concentration boundary layer thickness scaled by the layer depth $d$. With the above reasoning the dimensionless amplitude functions of disturbances, based on the relation (8), are assumed to have the form of

$$[w_1,\phi_1,\theta_1]=\lfloor\tau w^*(\zeta),\phi^*(\zeta),\theta^*(\zeta)\rfloor\exp[\mathrm{i}(a_x x+a_y y)], \tag{9}$$

where $\zeta=z/\sqrt{\tau}$, and $a_x$ and $a_y$ are the dimensionless wave numbers in $x$- and $y$-directions, respectively. The similarity variable $\zeta$ is introduced to take into account the position and temporal dependencies of disturbances. By using the relation (9) the following new set of dimensionless stability equations are obtained:

$$(D^2 - a^{*2})^2 w^* = \frac{1}{Sc}\left(-\frac{1}{2}\zeta D^3 + \frac{1}{2}a^{*2}\zeta D - a^{*2}\right)w^* + a^{*2}(\phi^* - Le\theta^*), \quad (10)$$

$$\left(D^2 + \frac{1}{2}\zeta D - a^{*2}\right)\phi^* = Rs^* w^* D\phi_0, \quad (11)$$

$$\left(D^2 + \frac{1}{2Le}\zeta D - a^{*2}\right)\theta^* = -\frac{Ra^*}{Le}w^* \quad (12)$$

with boundary conditions:

$$w^* = Dw^* = \phi^* = \theta^* = 0 \quad \text{for } \zeta = 0 \text{ and } \zeta \to \infty, \quad (13)$$

where $a^* = a\sqrt{\tau}$, $a = \sqrt{a_x^2 + a_y^2}$, $Rs^* = Rs\tau^{3/2}$, $Ra^* = Ra\tau^2$ and $D = \mathrm{d}/\mathrm{d}\zeta$. These equations involve time-dependent properties implicitly. It is assumed that $a^*$, $Ra^*$ and $Rs^*$ are all eigenvalues and the principle of exchange of stabilities is kept. For a given $Sc$, $Le$, $a^*$ and $Ra^*$ the minimum value of $Rs^*$ will be found numerically.

### 2.3. Solution method

In order to integrate the stability equations, Eqs. (10)–(12), trial value of the eigenvalue $Rs^*$ and the boundary conditions $D^3w^*$, $D\phi^*$ and $D\theta^*$ at $\zeta = 0$ are assumed properly for given $Sc$, $Le$, $a^*$ and $Ra^*$. Here the value of $Sc$ and $Le$ are fixed at 2100 and 300, respectively, in order to consider double diffusion of heat and copper ion in aqueous sulfuric acid and copper sulfate solution. Since boundary conditions represented by Eq. (13) are all homogeneous, the value of $D^2w^*$ at $\zeta = 0$ can be assigned arbitrarily. This procedure is based on the outward shooting method in which the boundary value problem is transformed into the initial value problem. The trial values, together with the four known conditions at lower boundary, give all the information to make numerical integration. The integration based on the fourth-order Runge–Kutta method is performed from $\zeta = 0$ to fictitious distance to satisfy the infinite boundary conditions. By using the Newton–Raphson iteration the trial value of $Rs^*$, $D^3w^*$, $D\phi^*$ and $D\theta^*$ are corrected until the stability equations satisfy the infinite boundary conditions within the maximum relative tolerance of $10^{-8}$. Then, by increasing the distance step by step, the above integration is repeated. Finally, the value of $Rs^*$ is decided through the extrapolation.

### 2.4. Stability analysis results

The resulting neutral stability curves calculated with changing values of $a^*$ and $Rs^*$, are shown in Fig. 3. According to the present theory the minimum value of $Rs^*$ and $a^*$ can be obtained for a given $Ra^*$, as shown in Fig. 3, and it characterizes the critical condition of convective motion. By using the relation of $Rs_c^* = Rs\sqrt{\tau_c^3}$ and $Ra_c^* = Ra\tau_c^2$, we can determine the critical time $\tau_c$ for given $Rs$ and $Ra$.

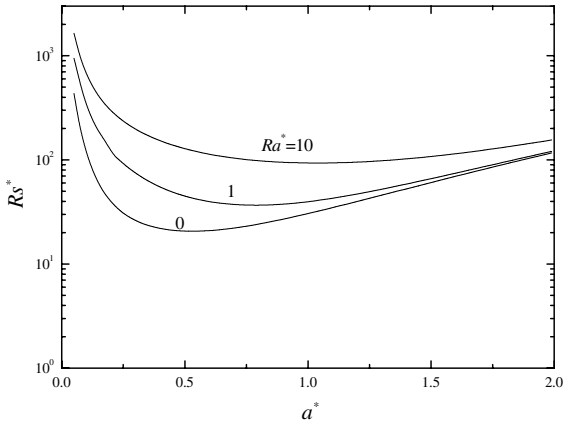


Fig. 3. Neutral stability curves for $Sc = 2100$ and $Le = 300$ for various $Ra^*$.

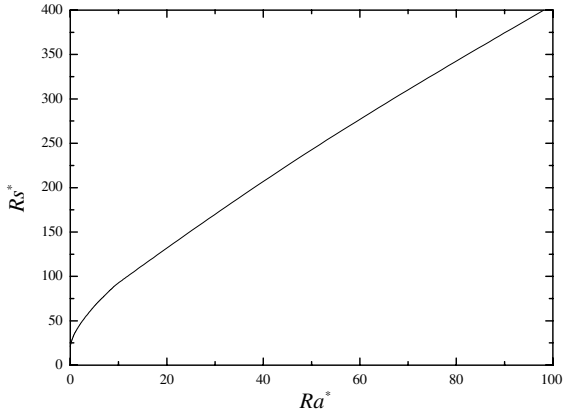


Fig. 4. Critical condition of double-diffusive convection.

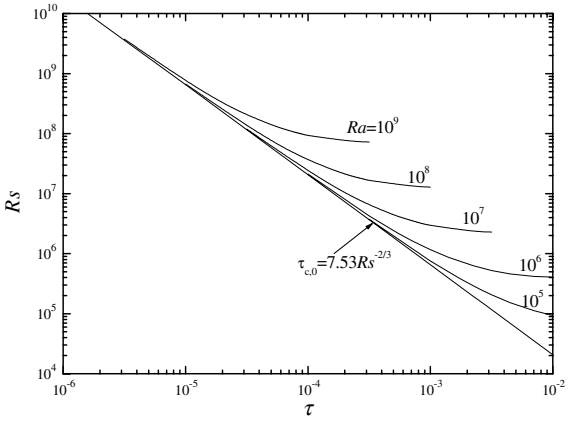


Fig. 5. Effect of $Ra$ on the critical time for a given $Rs$.

Fig. 4 shows that the onset time is delayed as $Ra$ increases for given $Sc$, $Le$ and $Rs$. The effect of the temperature gradient on the critical time is summarized in Fig. 5. The minimum bound of Fig. 5, i.e. $\tau_{c,0} = 7.53Rs^{-2/3}$ corresponds to the case of the zero temperature gradient of $Ra = 0$. Recently, Bograchev et al. [18] suggested the similar relation of $\tau_{c,0} = 2.4Rs^{-2/3}$. The thermal stabilizing effect begins to be observable at approximately $Rs \leqslant 0.01LeRa$. And, for the base state of linear profiles, i.e. for the fully developed state of $\tau \to \infty$, the stability conditions can be approximated by [2]

$$Rs_c - Ra = 1708 \text{ with } a_c = 3.117 \quad \text{for } \tau \to \infty. \tag{14}$$

## 3. Experiments

### 3.1. Experimental setups

The system of double-diffusive convection employed in the present investigation is that of the electrochemical redox reaction of copper ion in aqueous copper sulfate solution with stable thermal stratification. The present double-diffusive system is schematized in Fig. 1. This electrochemical system has been widely used in studying buoyancy-driven phenomena as copper sulfate has a reasonable solubility in water and does not form soluble product on the electrode surface [19]. Copper plates were used as both cathode and anode. At the cathode following reduction reaction occurs:

$$Cu^{2+} + 2e^- \to Cu,$$

while the following oxidation reaction proceeds at the anode:

$$Cu \to Cu^{2+} + 2e^-.$$

In these experiments sulfuric acid was added as a supporting electrolyte to lessen the migration effect.

The dependency of density, viscosity and mass diffusivity on composition were calculated by using the following correlations:

$$\rho(\mathrm{g\ cm^{-3}}) = 0.9978 + 0.06406M_{H_2SO_4} - 0.00167M^2_{H_2SO_4} + 0.122755M_{CuSO_4} + 0.01820M^2_{CuSO_4},$$

$$\mu(\mathrm{cp}) = 0.974 + 0.1235M_{H_2SO_4} + 0.0556M^2_{H_2SO_4} + 0.5344M_{CuSO_4} + 0.5356M^2_{CuSO_4},$$

$$\mu \cdot \alpha_s(\mathrm{cm^2\ s^{-1}}) = (0.7363 + 0.00511M_{H_2SO_4} + 0.02044M_{CuSO_4}) \times 10^{-5},$$

which were suggested by Fenech and Tobias [20] for 22 °C within the error bounds of 0.5%. The temperature effects on these physical properties were calculated by following Chiang and Goldstein's work [21].

The electrochemical cell was constructed as a cubic with two horizontal copper plates with the same area of $5 \times 5\ \mathrm{cm^2}$ and four vertical acrylic plates with various depths of 3, 4 and 5 cm. The fluid layer is initially quiescent at a constant concentration $C_b$ and stably stratified by a uniform temperature gradient. For the stable temperature gradient, the upper surface was heated uniformly while the lower one was cooled by circulating constant temperature water through the copper plates. The electrolyte consists of 0.03–0.3 M $CuSO_4$ solutions with 1.5 M $H_2SO_4$ as a supporting electrolyte. Copper ion was deposited on the cathode electrode under the limiting current condition, and was dissolved from the anode one. The electrical information in the cell were obtained by a PC controlling potentiostat (EG&G Parc.) on line. The calomel reference electrode was used to measure the potential difference between the electrolyte solution and the cathode. The experimental setup is given in Fig. 6.

Ionic mass transfer experiments were carried under the limiting current condition in horizontal electrolyte solution. The typical limiting current under the typical condition is shown in Fig. 7. As the potential difference increase, the current flowing between the two electrodes increase sharply at first until the limiting potential difference reaches a certain value. However, above this potential difference the current rise again. At this stage, the hydrogen ions take part in electrochemical reaction and hydrogen gas bubbles evolve. The plateau where an increase in potential difference causes almost no increase in current is known as the limiting current. Experiments were repeated separately in two different modes of unstable (cathode facing upward) buoyancy-driven convection or stable (cathode facing downward) diffusion for various thermal gradients, cell depths and concentrations of bulk solution. Typical current–time curve is shown in Fig. 8. Two curves are coincident each other to a certain point, where buoyancy-driven motion sets in for unstable geometry. The upside down S-shape of current variations with time shows the peculiar behavior of natural convection in an ionic mass transport. It is

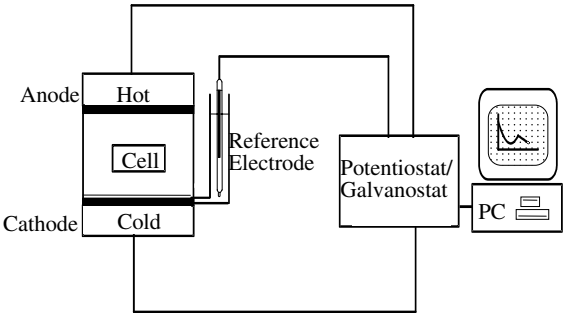


Fig. 6. Experimental setup.

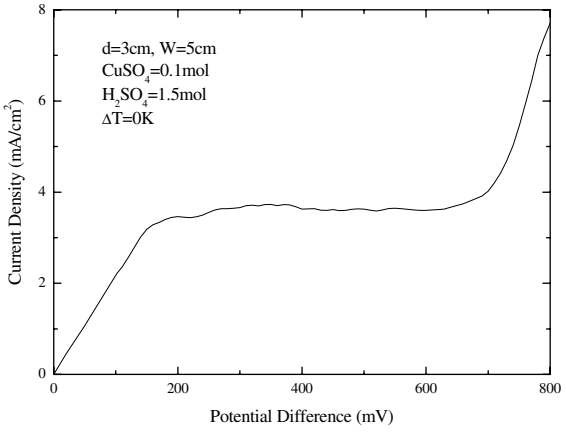


Fig. 7. Typical limiting current curve.

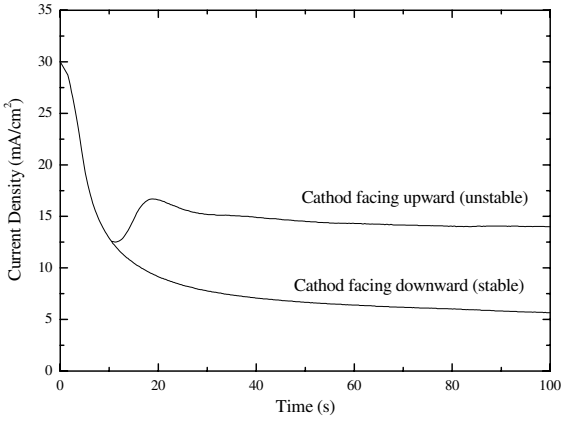


Fig. 8. Current–time behaviors of stable and unstable geometries.

considered that convective flows start at the minimum point of each current curve in a detectable manner.

### 3.2. Experimental results and discussions

Patrick and Wragg [22], Inoue et al. [23] and Morgunova et al. [24] measured the individual mass transfer coefficient with time in electroplating system, where $Sc > 2000$. Their undershoot time which indicates the minimum of the Sherwood number $Sh$ in the plot of $Sh$ vs. $\tau$ and is assumed to be marked the characteristic time to exhibit the mass transfer enhancement due to natural convection is shown in Fig. 9. In this limiting case the Lewis number and thermal Rayleigh number do not affect the critical time, and the present values of $\tau_c$ are about one fourth of the experimental undershoot time.

Foster [25] commented that with correct dimensional relations the relation of $\tau_0 \cong 4\tau_c$ would be kept for the

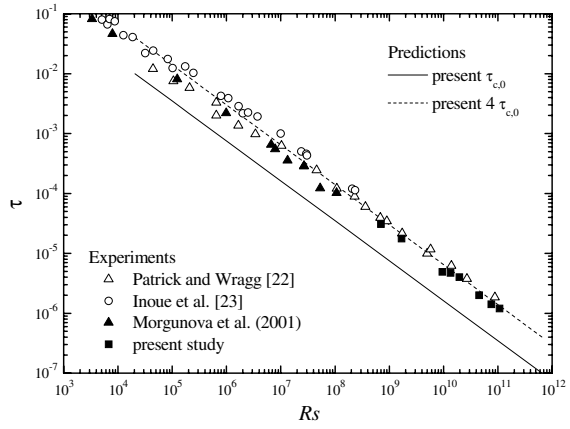


Fig. 9. Comparison of present predictions with experimental data of $Ra = 0$.

case of horizontal fluid layers heated isothermally from below. This means that the growing time for disturbances is needed before they are detected experimentally. Therefore, it seems evident that the predicted onset time $t_c$ is smaller than the detection time $t_0$. This means that a fastest growing mode of instabilities, which set in at $t = t_c$, will grow with time before manifest motion is first detected experimentally. For deep-pool systems, $4\tau_c$ represents manifest convection very well. This may support Foster's viewpoint that the predicted onset time of convection motion with correct dimensionless relations would be too early by a factor of about 4 [25].

The effect of stable thermal stratification on the onset time of buoyancy-driven convection is characterized experimentally and summarized in Fig. 10. The range of thermal Rayleigh number in this experiment is

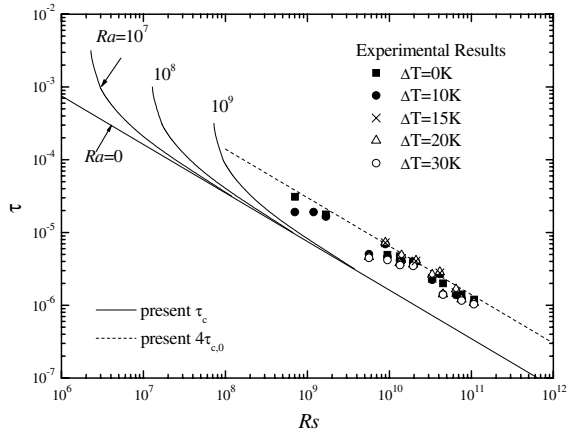


Fig. 10. Comparison of predictions with experimental data. The range of thermal Rayleigh number in this experiment is $2 \times 10^6 \leqslant Ra \leqslant 4 \times 10^8$.

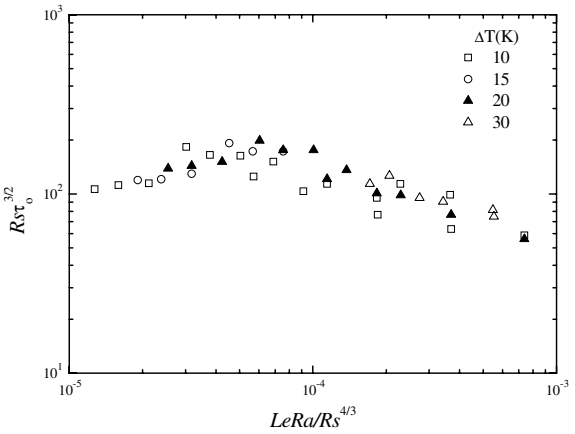


Fig. 11. Effect of degree of initial stratification, $LeRa/Rs^{4/3}$ on the onset time.

$2\times10^6 \leqslant Ra \leqslant 4\times10^8$. As shown in this figure, as the magnitude of stable thermal stratification increase the onset time decrease. This is an unexpected result and opposite to the theoretical result that stable thermal stratification delays the onset time of convection. The effect of stable stratification on the onset of convective motion is described in Fig. 11. As shown in this figure, for the range of $LeRa/Rs^{4/3} \leqslant 5\times10^{-5}$ it may be stated that for a given $Rs$ convective motion is detected earlier with increasing $LeRa/Rs^{4/3}$. This trend is reversed for the region of $LeRa/Rs^{4/3} > 5\times10^{-5}$, that is the stable stratification accelerates the onset of convection. Similar trend was observed in Ueda et al.'s [26] experimental and theoretical results.

Ueda et al.'s system is an initially stably stratified, horizontal fluid layer of thickness $d$. For time $t \leqslant 0$, the conduction field has a linear temperature profile with $T = T_i$ at the vertical distance $Z = 0$ and $T = T_u(>T_i)$ at $Z = d$. The fluid layer is heated from below with a higher temperature $T_b(>T_i)$ for $t > 0$. Their system is slightly different from the present one, but conceptually identical. In their system, the stable stratification delays or accelerates the onset of convective motion according to the degree of relative initial stratification, $\gamma = (T_u - T_i)/(T_b - T_i)$. They owed this unexpected trend to the multiple cell pattern at the onset of convective motion, even though it could not detect in their experiment. Recently, Choi et al. [27] reconsidered Ueda et al.'s system by solving Navier–Stoke and energy equations employing the nonlinear effects numerically. They introduce disturbances having very small amplitude at $t = 0$, and track the temporal growth of disturbance energy. According to their theoretical results, the convective motion is onset at the time predicted by propagation theory which is employed in the present study, and the growth period is required to the disturbances are amplified to be detected experimentally. In their study, for a certain range of stable stratification, the growth period becomes short as the degree of stratification becomes intensified. The present results seem to be explained by considering the growth period of the disturbances, i.e. for the range of $LeRa/Rs^{4/3} > 5\times10^{-5}$ the growth period is shortened as the stable stratification becomes intensified.

## 4. Conclusions

The onset of double-diffusive convection in a horizontal fluid layer with stable thermal stratification is investigated theoretically and experimentally. For the limiting case of $Ra = 0$, i.e. no initial stable stratification, the stability criteria compare reasonably well with experimental results and manifest convection seems to be observable. In the single diffusion case of $Ra = 0$, the velocity disturbances look too weak to be observable experimentally for $\tau \leqslant 4\tau_c$. The detection time of double-diffusive convection was delayed or accelerated depending on the degree of initial stratification, $LeRa/Rs^{4/3}$. For the range of $LeRa/Rs^{4/3} > 5\times10^{-5}$ the detection time is shortened as the stable stratification becomes intensified. This unexpected results could be explained by considering the time required for disturbances to grow and further studies on the growth of disturbances are required.

## Acknowledgement

This work was supported by the Nuclear Academic Research Program of the Ministry of Science and Technology (MOST).

## References

[1] S. Ostrich, Fluid mechanics in crystal growth—the 1982 Freeman Scholar Lecture, J. Fluid Eng. 105 (1983) 5–20.
[2] J.S. Turner, Buoyancy Effects in Fluids, Cambridge University Press, Cambridge, 1973.
[3] C.F. Chen, D.H. Johnson, Double-diffusive convection: a report on an engineering foundation conference, J Fluid Mech. 138 (1984) 405–416.
[4] D.A. Nields, The thermo-haline Rayleigh–Jeffrys problem, J. Fluid Mech. 29 (1967) 545–548.
[5] M. Kaviany, M. Vogel, Effect of solute concentration on the onset of convection: uniform and nonuniform initial gradients, Trans. ASME: J. Heat Transfer 108 (1986) 776–782.
[6] D.Y. Yoon, C.K. Choi, C.G. Lee, M.C. Kim, U. Choi, The onset of double-diffusive convection in a stably stratified fluid layer heated from below, Korean J. Chem. Eng. 13 (1996) 15–20.
[7] T.D. Foster, Stability of homogeneous fluid cooled uniformly from above, Phys. Fluids 8 (1965) 1249–1257.

[8] M. Kaviany, Onset of thermal convection in a fluid layer subjected to transient heating from below, Trans. ASME: J. Heat Transfer 106 (1984) 817–823.
[9] M.C. Kim, T.J. Chung, C.K. Choi, Onset of buoyancy-driven convection in the horizontal fluid layer heated from below with time-dependent manner, Korean J. Chem. Eng. 21 (2004) 69–74.
[10] C.K. Choi, T.J. Chung, M.C. Kim, Buoyancy effects in the plane Couette flow heated uniformly from below with constant heat flux, Int. J. Heat Mass Transfer 47 (2004) 2629–2636.
[11] C.K. Choi, J.H. Park, M.C. Kim, J.D. Lee, J.J. Kim, E.J. Davis, The onset of convective instability in a horizontal fluid layer subjected to a constant heat flux from below, Int. J. Heat Mass Transfer 47 (2004) 4377–4384.
[12] I.G. Hwang, C.K. Choi, Onset of compositional convection during solidification of a two-component melt from a bottom boundary, J. Cryst. Growth 267 (2004) 714–723.
[13] K.H. Kang, C.K. Choi, A theoretical analysis of the onset of surface-tension-driven convection in a horizontal liquid layer cooled suddenly from above, Phys. Fluids 9 (1997) 7–15.
[14] K.H. Kang, C.K. Choi, I.G. Hwang, Onset of solutal Marangoni convection in a suddenly desorbing liquid layer, AIChE J. 46 (2000) 15–23.
[15] M.C. Kim, C.K. Choi, The onset of Taylor–Görtler vortices in impulsively decelerating swirl flow, Korean J. Chem. Eng. 21 (2004) 767–772.
[16] M.C. Kim, T.J. Chung, C.K. Choi, The onset of Taylor-like vortices in the flow induced by an impulsively started rotating cylinder, Theor. Comput. Fluid Dyn. 18 (2004) 105–114.
[17] M.C. Kim, C.K. Choi, The onset instability in the flow induced by an impulsively started rotating cylinder, Chem. Eng. Sci. 60 (2005) 599–608.
[18] D.A. Bograchev, V.M. Volgin, A.D. Davydov, Non-steady-state processes under conditions of natural convection in an electrochemical cell with horizontal electrodes: the critical time of the onset of a convective instability at large Rayleigh numbers, Russ. J. Electrochem. 40 (2004) 558–562.
[19] R.J. Goldstein, H.D. Chiang, D.L. See, High-Rayleigh-number convection in a horizontal enclosure, J. Fluid Mech. 213 (1990) 111–126.
[20] E.J. Fenech, C.W. Tobias, Mass transfer by free convection at horizontal electrodes, Electrochim. Acta 2 (1960) 311–325.
[21] H.D. Chiang, R.J. Goldstein, Application of the electrochemical mass transfer technique to the study of buoyancy-driven flows, in: Proceedings of 4th International Symposium on Transport Phenomena in Heat and Mass Transfer, Sydney, vol. 1, 1991, pp. 1–25.
[22] M.A. Patrick, A.A. Wragg, Optical and electrochemical studies of transient free convection mass transfer at horizontal surfaces, Int. J. Heat Mass Transfer 18 (1975) 1397–1407.
[23] Y. Inoue, S. Akutagawa, S. Saeki, R. Ito, Bénard convection of electrolytic solution in electric field, Kagaku Kokaku Ronbun. 9 (1983) 359–369.
[24] E.E. Morgunova, L.A. Reznikova, A.P. Grogon, A.D. Davydov, Convective instability of the triiodide reduction in an electrolyte cell with horizontal electrodes, Russ. J. Electrochem. 37 (2001) 982–986.
[25] T.D. Foster, Onset of manifest convection in a layer of fluid with a time-dependent surface temperature, Phys. Fluids 12 (1969) 2482–2487.
[26] H. Ueda, S. Komori, T. Miyazaki, H. Ozoe, Time-dependent thermal convection in a stably stratified fluid layer heated from below, Phys. Fluids 27 (1984) 2617–2623.
[27] C.K. Choi, J.H. Park, H.K. Park, H.J. Cho, T.J. Chung, M.C. Kim, Temporal evolution of thermal convection in an initially, stably stratified fluid, Int. J. Thermal Sci. 43 (2004) 817–823.